## Design and evaluation of a multiplexed angular-scanning surface plasmon resonance system employing line-laser optics and CCD detection in combination with multi-ligand sensor chips

Lakayan, Dina; Tuppurainen, Jussipekka; Eemeli Suutari, Teemu; van Iperen, Dick J.; Somsen, Govert W.; Kool, Jeroen

***published in***
Sensors and Actuators, B: Chemical
2019

***DOI (link to publisher)***
10.1016/j.snb.2018.11.046

***document version***
Publisher's PDF, also known as Version of record

Sensors & Actuators: B. Chemical 282 (2019) 243–250

Contents lists available at ScienceDirect

Sensors and Actuators B: Chemical

journal homepage: www.elsevier.com/locate/snb

# Design and evaluation of a multiplexed angular-scanning surface plasmon resonance system employing line-laser optics and CCD detection in combination with multi-ligand sensor chips

Dina Lakayan[a,b], Jussipekka Tuppurainen[c], Teemu Eemeli Suutari[a,d], Dick J. van Iperen[e], Govert W. Somsen[a], Jeroen Kool[a,*]

[a] Division of BioAnalytical Chemistry, Amsterdam Institute for Molecules, Medicines and Systems, Department of Chemistry and Pharmaceutical Sciences, Faculty of Science, Vrije Universiteit Amsterdam, Amsterdam, the Netherlands
[b] TI-COAST, Science Park 904, 1098 XH Amsterdam, the Netherlands
[c] BioNavis Ltd., Tampere, Finland
[d] Centre for Drug Research, Division of Pharmaceutical Biosciences, Faculty of Pharmacy, University of Helsinki, P.O. Box 56, 00014 Helsinki, Finland
[e] Fine Mechanical Instrumentation and Engineering Group, Faculty of Science, Vrije Universiteit Amsterdam, the Netherlands

ARTICLE INFO

*Keywords:*
Multiplexing
Angular-scanning SPR
Antibody-protein interaction

ABSTRACT

An angle-scanning Kretschmann configuration SPR instrument allowing multiplexed analysis is presented. Laser light was guided through optics that converted the collimated light into a line-shaped beam, which was directed to a prism, illuminating the gold sensor surface over a 1 × 10 mm area. The reflected light was led to a CCD detector providing simultaneous readout of individual analysis spots along the laser line at a selected angle (fixed-angle detection) or in scanning-angle mode (width of 35°). Full SPR curve could be measured every 3.6 s for each illuminated spot on the sensor surface. Two in-house manufactured flow cell designs were used for evaluating multiplexed angular-scanning SPR. The first comprised six parallel channels with the laser line perpendicular to the flow direction in order to allow interrogation of the sensor surface in the six channels. Refractive index changes by varying solution composition, and adsorption of different concentrations of albumin to the sensor surface could be correctly monitored simultaneously in each of the channels. In the second flow-cell design the laser line was coinciding with the flow path, allowing recording of SPR curves along a 10-mm length of the sensor surface. Adsorption of layers of positively and negatively charged polyelectrolytes could be consistently measured for sixteen selected positions along the channel. As a proof of principle, several target proteins were immobilized on different positions along the sensor and the binding of various antibodies with these proteins was monitored simultaneously, showing excellent selectivity and reproducibility for probing antibody-protein interactions in a multiplexed fashion.

## 1. Introduction

Label-free optical biosensors have found a vast range of applications in life sciences [1]. Among these sensing techniques, surface plasmon resonance (SPR) spectroscopy has extensively been used for real-time assessment of biomolecular interactions. Most conventional SPR setups utilize a Kretschmann configuration comprising a prism coupler with a thin gold layer as a sensor, a He-Ne laser for plasmon excitation, and a photodetector [2]. This allows measurement of shifts in resonance angle caused by analyte binding to ligands immobilized on the sensor surface. SPR instruments mostly comprise only a limited number of flow channels [3,4], putting constraints on sample throughput. In situations where, for example, libraries of molecules have to be screened for binding against multiple target proteins, higher throughput SPR detection is in demand. The gain in throughput can be achieved by measuring multiple binding events simultaneously, e.g. by having multiple ligands immobilized on the surface of the SPR sensor and/or by having the possibility to measure more samples in parallel.

Multiplex SPR detection has been achieved with imaging SPR (iSPR) [5,6]. iSPR is usually performed in fixed angle mode with a charge-coupled device (CCD) camera used as a detector, capturing the reflected light modulation on the entire sensorchip [7,8]. These intensity changes

* Corresponding author at: Vrije Universiteit Amsterdam, Faculty of Sciences, AIMMS Division of BioAnalytical Chemistry, De Boelelaan 1085, 1081 HV Amsterdam, the Netherlands.
*E-mail address:* j.kool@vu.nl (J. Kool).

https://doi.org/10.1016/j.snb.2018.11.046
Received 28 August 2018; Accepted 8 November 2018
Available online 13 November 2018

can be monitored for regions of interest (ROIs) in real time through the entire sensor, allowing simultaneous, continuous observation of several interactions (multiplexing) on the surface of sensor chip. These interactions are displayed in a sensorgram at the same time of monitoring. Multiplex SPR detection providing monitoring of angular shifts over a limited range has been introduced [9–12], employing a scanning mirror directly after the light source, enabling scanning of the incidents angle over 8° [13–19].

In this study, multiplexed analysis employing an angular-scanning SPR instrument facilitating the simultaneous recording of full SPR curves with a width of 35° for multiple spots and analytes is developed and explored. For that, hardware modifications were implemented, including optics stretching the narrow laser beam into a uniform light line, and use of a CCD camera for real-time detection reflected laser light detection from multiple positions. In addition, dedicated software was used to convert the measured light intensities of selected areas on the sensor to full SPR curves. For the fluidic part of the system, two new flow cells were designed and produced in-house. One comprises six horizontal channels in order to allow SPR assessment of six different solutions simultaneously. The other flow cell has a single channel that is interrogated by the laser line over a 1-cm distance. The position of each of the six flow channels or the ROIs in the single channel flow cell is defined by the CCD software, permitting monitoring of reflected-light intensity changes at variable angles for the selected areas.

The performance of the newly designed systems was step-wise evaluated. First, the responsiveness to bulk refractive index changes at the sensor surface was checked by monitoring SPR curves of air or different solvents. Next, the potential of the multiplexed system for probing analyte adsorption to the gold sensor surface was tested by applying different concentrations of the protein albumin as well as layers of oppositely-charged polyelectrolytes while simultaneously recording SPR curves of different locations. Detection of protein binding to polyelectrolyte layers on the sensor surface was also investigated. As a final proof of concept, target proteins were immobilized in separated spots in one single channel and the interaction of three antibodies for the target proteins was studied in a multiplexed fashion by SPR.

## 2. Experimental

### 2.1. Hardware

A schematic of the optical and fluidic design changes made for allowing multiplexed analysis are shown in Fig. 1. SPR analyses were performed using an internally adapted multi-parametric SPR Navi 200 instrument from BioNavis Ltd. (Tampere, Finland). The collimated laser beam (670 or 785 nm) was adopted to a line (1 × 10 mm) using line generating optics (Fig. 1a). The laser light was directed at variable angle through the glass prism towards the SPR sensor. The intensity of reflected light was monitored using a CCD camera as detector. An algorithm was developed and implemented in the BioNavis software for rapid processing of the obtained CCD camera images. The algorithm converts the light intensity levels of selected ROIs to an output signal, which is plotted as a function of the incident angle, providing SPR curves for each of the selected ROIs on the sensor chip. A fluidic design with six horizontal flow channels (Fig. 1b) and another with one vertical channel (Fig. 1c) were produced fitting the BioNavis setup. For immobilization of 16 spots evenly positioned in line on the sensor surface, a silicon mask (Fig. 1d) was produced in-house.

The flow cells were produced in-house by an advanced DMU/DMC monoBLOCK® series milling machine, (Veenendaal, the Netherlands). Dow Corning 184 PDMS (Dow Corning Europe, Seneffe, Belgium) was used to seal the flow cells and was first degassed in a desiccator. For connection pieces of tubing (IDEX 1581, PEEK, 0.1 × 1/32 × 5, FT, BLUE) were placed at the inlets and outlets of the flow channels. To avoid blockage of the tubing during PDMS backing, core wires were inserted. The tubing was fixed with Loctite M-121HP Hysol Medical Device Epoxy Adhesive (Henkel KGaA, Dusseldorf, Germany). The tubing was secured with micro tights (IDEX F-126HX, 1-PIECE Micro Tight, HEADLESS, 6-3, 1/32 IN, peek, red). The flow cell was then baked in an oven for 120 min at 100 °C followed by cooling to room temperature. The six individual fluidic channels were 5.7 mm in length, 0.6 mm in width, and 1.5 mm in depth. The single flow channel had a width of 2.65 mm, a length of 10.5 mm and a depth of 0.33 mm.

The silicone mask was designed and produced in-house. The Dow Corning 184 Silicone Elastomer used for this (Dow Corning Europe, Seneffe, Belgium) was first degassed in a desiccator at 1 mbar for 30 min. The mold was then filled with the degassed Dow elastomer and baked in an oven for 120 min at 100 °C. Next, the mask with mold was cooled to room temperature after which the mask was removed from the mold. Finally, the mold was cut to exactly fit the BioNavis sensor holder.

### 2.2. Chemicals and reagents

Sodium chloride (NaCl), poly sodium 4-styrenesulfonate (PSS), poly allylamine hydrochloride (PAH), polyethylenimine (PEI), 2-(N-morpholino)ethanesulfonic (MES) monohydrate, human serum albumin (HSA), human hemoglobin, transferrin, cytochrome c from bovine heart, anti-human albumin antibody produced in rabbit, anti-human hemoglobin antibody produced in rabbit, anti-myoglobin antibody produced in rabbit, phosphate buffered saline (PBS), ethanolamine hydrochloride, L-cysteine, N-hydroxy succinimide (NHS), N-(3-

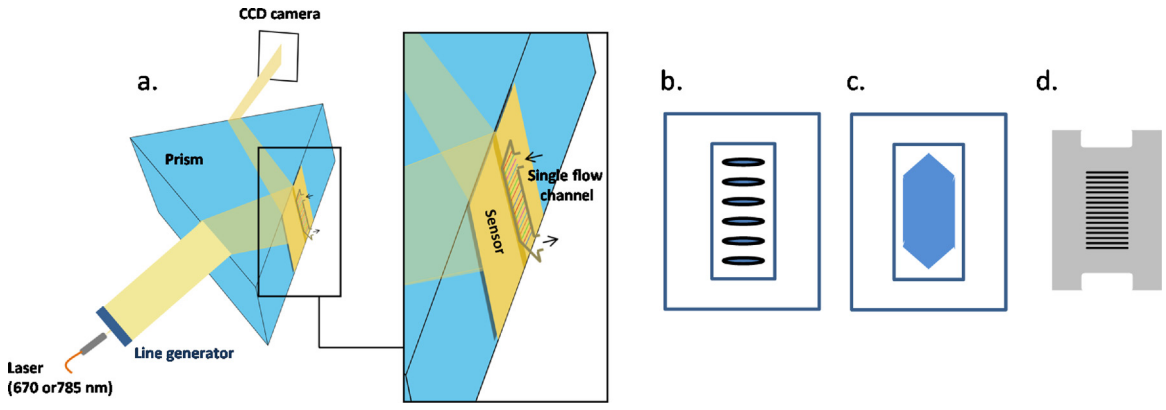


**Fig. 1. a.** Schematic of the optical setup for multiplexing SPR. The produced laser line probes the entire length of the surface of the sensor chip covered by the single flow channel. The reflected line is projected on and imaged by the CCD camera detector. The zoomed view of the sensor slide shows the positioning of the single flow cell setup with 16 line-shaped spots on the sensor chip surface. **b.** Six flow-channel format. **c.** Single flow-channel format. Immobilization of multiple compounds on the sensor surface was done online when using the six flow-channel cell or **d**. offline when using the single flow-channel cell using the silicon mask.

dimethylaminopropyl)-N'-ethylcarbodiimide hydrochloride (EDC) and sodium hydroxide (NaOH) were purchased from Sigma-Aldrich (Steinheim, Germany). Deionized water was produced by a Milli-Q purification system from Millipore (Amsterdam, the Netherlands). Dulbecco's phosphate-buffered saline (DPBS) was from Gibco, Thermo Fisher Scientific (Massachusetts, USA).

### 2.3. Multiplexed SPR using the six-channel flow cell

An integrated SPR Navi peristaltic pump of the SPR device was used for two of the fluidic channels, whereas a Gilson minipuls-2 L4 peristaltic pump (Middleton, USA) was used for the remaining four channels. The flow rate was 30 µl/min for all channels, and the SPR temperature was 24 °C. All measurements were performed with the 785-nm laser in combination with gold (Au) sensor chips (from BioNavis). The system was tested for air, Milli-Q water and ethanol. In addition, HSA (0, 0.03, 0.1, 0.3, 1.0 and 3.0 mg/mL) in Dulbecco's phosphate-buffered saline (DPBS), were analysed.

### 2.4. Multiplexed SPR using the single channel flow cell

All the measurements were performed with Au sensor chips and the 785-nm laser.

#### 2.4.1. Online immobilization of polyelectrolytes

The flow rate was 50 µL/min and the flow cell temperature was 20 °C. After obtaining stable baselines for all the ROIs using 0.15 M NaCl as running solvent, the surface was cleaned twice with a 5% Hellmanex solution for 4 min. Polyelectrolytes were deposited successively via plug-injections (4 min each) of solutions containing 0.1 mg/ml PEI, 0.1 mg/ml PSS and 0.1 mg/ml PAH (all in running solution), respectively. After each experiment, the sensor surface was regenerated using a 5% hellmanex solution plug-injection for 4 min.

#### 2.4.2. Offline immobilization of polyelectrolytes

The surface of the sensor chip was cleaned by pipetting 5% Hellmanex solution over the complete surface of the sensor chip and incubating for 4 min. The sensor chip was then rinsed with 0.15 M NaCl. Next, the sensor chip was incubated with solutions of 0.1 mg/ml PEI followed by 0.1 mg/ml PSS (both in 0.15 M NaCl), each solution for 4 min covering. For exposing only half of the sensor chip to polyelectrolyte, half of the Au surface was covered with tape, followed by pipetting 0.1 mg/ml PAH in 0.15 M NaCl over the non-covered half of the sensor chip. After immobilization, the sensor chip was put in a BioNavis holder and inserted into the SPR instrument. The sensor temperature was set at 20 °C. After obtaining a stable baseline (usually within 2–4 min), analyses were initiated. As a test experiment, 1 mg/ml lysozyme (in 0.15 *M* NaCl) was plug-injected at a flow rate of 50 µL/min.

### 2.5. Probing protein-antibody interactions by multiplexed SPR

#### 2.5.1. Offline protein immobilization

For protein immobilization, a carboxymethyl dextran (CMD) hydrogel gold sensor chip (BioNavis) was first activated with a solution containing 0.2 M EDC and 0.1 M NHS in water at room temperature for 10 min by pipetting the solution over the entire surface of the sensor chip. The surface was then washed with 5 mM of MES hydrochloride (adjusted to pH 4 with NaOH) and dried under a gentle nitrogen stream. The sensor chip was then positioned in the sensor chip holder for offline immobilization, and the in-house developed silicon mask (Fig. 1d) with sixteen slit-shaped openings was tightly placed over the surface of the sensor chip. Immobilization of proteins was done by pipetting their solutions into the individual slits using a 1-µl Agilent syringe needle followed by incubation, deactivation and washing steps standard to EDC activated CMD immobilizations for SPR.

#### 2.5.2. Antibody-protein binding analysis (direct assay)

After protein immobilization, the sensor chip in the holder was placed in the SPR instrument. On the sensor chip, five spots (length, 0.3 mm) of HSA, five hemoglobin, two transferrin, two cytochrome c and two blank spots (reference) were positioned along one line with an inter-spot distance of 0.3 mm. The locations of the immobilized proteins were specified by the software. SPR analyses were done in angular-scan mode using the 785-nm laser. The in-house developed single-channel flow cell was used to direct plug-injections of samples to the spots on the SPR sensor chip. PBS buffer (containing 0.01 M phosphate with 2.7 mM potassium chloride and 0.137 M sodium chloride (pH 7.4)) was used as running buffer at a flow rate of 30 µL/min with a sensor cell temperature of 20 °C. After obtaining a stable baseline, 0.1–100 µg/mL anti-HSA triplicate plug-injections were performed followed by triplicate plug-injections of 0.1–100 µg/mL anti-hemoglobin and then 0.1–100 µg/mL anti-myoglobin antibodies (all diluted in running buffer) for 7 min per plug-injection. For regeneration, a solution of 50 mM NaOH was plug-injected for 1 min. The resonance angle shifts in time for all monitored spots were plotted as sensorgrams. From these data, binding constants for the interactions were calculated with TraceDrawer™ for SPR Navi™ (Ridgeview Instruments AB, Vange, Sweden).

#### 2.5.3. Antibody-protein binding analysis (competitive assay)

An antibody or mixed antibodies were pre-incubated with their respective antigens at different concentrations and then analyzed by SPR. Potential cross-reactive and/or non-specific binding was assessed with HSA for hemoglobin and vice versa, and with transferrin, cytochrome c and blank reference spots as negative controls. First, a mixture of 100 µg/ml anti-HSA and 100 µg/ml anti-hemoglobin was incubated on ice for 30 min with 200 µg/ml HSA and 200 µg/ml hemoglobin. Then, the incubated mixtures were plug-injected for 7 min at a flow rate of 30 µl/min. Other analyses involved mixtures of 50 µg/ml anti-HSA and 100 µg/ml anti-hemoglobin pre-incubated with different concentrations of HSA and/or hemoglobin (0–200 µg/ml). From the data obtained, IC50 values were calculated using GraphPad PRISM Software (San Diego, CA, USA).

## 3. Results and discussion

A commercial benchtop angular-scanning SPR instrument was adapted for multiplexed analysis by introducing a line laser for excitation and a CCD camera for detection (Fig. 1a). Multiplexing was studied using a six-channel flow cell (Fig. 1b) and a single-channel flow cell (Fig. 1c). Custom-developed software allowed selection of ROIs. For that, the positions of the flow channels and the silicon mask openings were determined by monitoring the reflected light of the laser line over its entire length at the resonance angle for air (~43°). The positions where void flow channels or silicon mask openings are located show SPR (i.e. attenuated intensity), whereas the areas where the gold surface is covered by the flow cell or mask material, no resonance occurs (no change in intensity). After the selection of ROIs, the scanning angle is selected. While performing SPR analysis, the software determines an average signal for the selected ROIs as a function of incident angle, which is then plotted as SPR curves. From these the shifts in the SPR dip angle can be monitored in time, producing a sensorgram.

### 3.1. Basic performance of the multiplexed SPR setup

First experiments were carried out with the six flow-channel cell using a bare gold sensor surface. In order to check whether the introduced optics worked adequately and ROIs were selected properly, SPR curves were monitored for each channel filled with air or 0.15 M NaCl in water. The system allowed simultaneous monitoring of full SPR curves from each channel (Fig. 2a and b), showing similar and correct resonance angles for the respective media (~43.05° for air and ~68.60

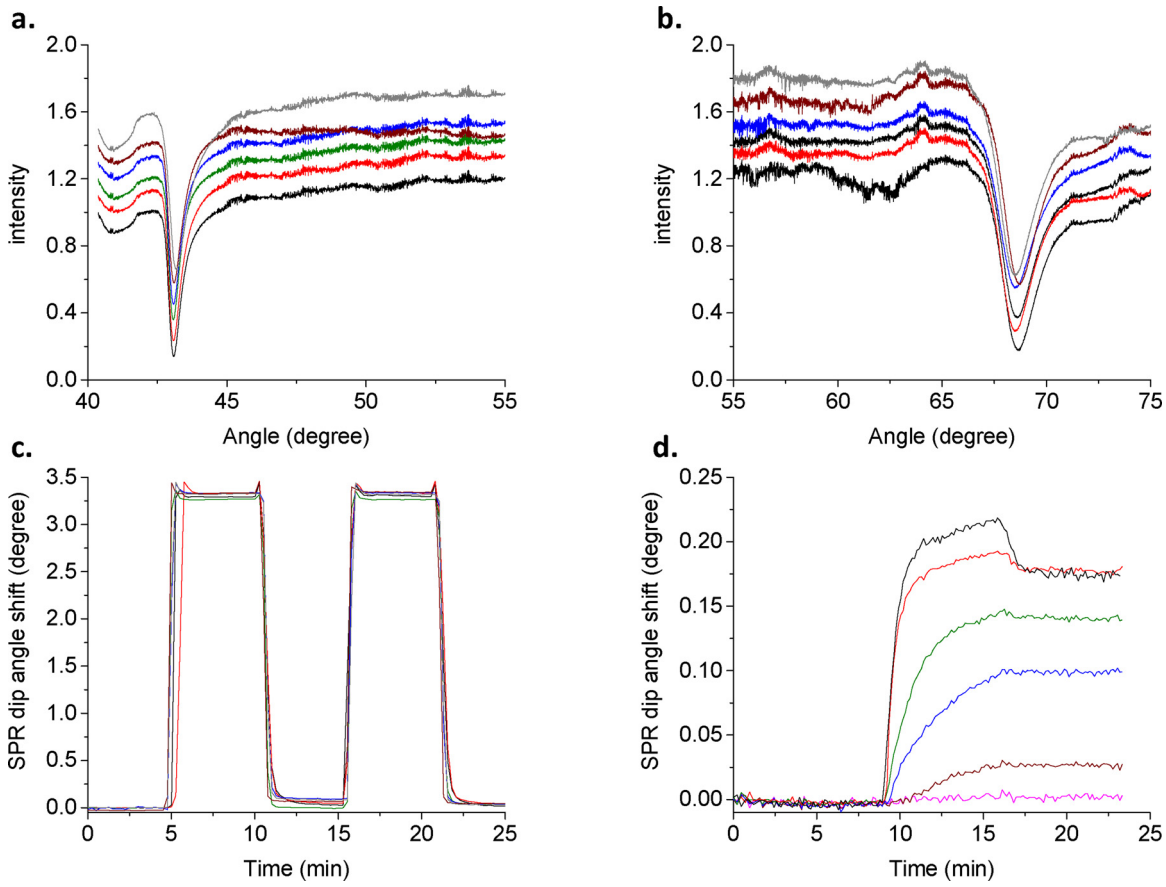


**Fig. 2.** Multiplexed angular scanning SPR using the six-channel flow channel and a bare gold sensor. The figures show the individual responses obtained for each respective channels. Full SPR curves obtained for **a.** air, **b.** water; curves were given an intensity offset for clarity (avoiding overlap). Sensorgrams (resonance angle shift vs. time) obtained for **c.** two consecutive plug-injections of ethanol using water as running liquid, and **d.** plug injections of HSA in water with each channel filled with a different concentration (0, 0.03, 0.1, 0.3, 1.0 and 3.0 mg/ml for channel 1 (pink), 2 (brown), 3 (blue), 4 (green), 5 (red), 6 (black), respectively. (For interpretation of the references to colour in this figure legend, the reader is referred to the web version of this article).

for the NaCl solution). Potential performance differences among the channels were evaluated by monitoring the SPR response caused by plugs of ethanol using water as running solvent. The shift in resonance angle caused by the change of the solvent's refractive index was properly monitored for all channels simultaneously, yielding very similar sensorgrams (Fig. 2c) and thus showing satisfactory inter-channel consistency. Each channel also exhibited excellent plug-to-plug repeatability (Fig. 2c). The multiplexing ability was further evaluated by analysis of HSA in water, plug-injecting different concentrations (0–3.0 mg/mL) into each of the six channels. The resulting sensorgrams nicely show the adsorption of HSA to the gold surface (Fig. 2d) with larger shifts observed for higher concentrations of HSA injected. At an injected concentration of 1 mg/ml and higher, the surface was saturated, as the same plateau signal was reached as for the 3.0-mg/mL solution. Overall, these results show that the new angular scanning SPR setup with line-laser optics and CCD detector allows simultaneous recording of correct SPR curves and sensorgrams from predefined spatially-separated areas on the sensor surface with good repeatability.

### 3.2. Single-channel multiplexed SPR

Further evaluation of the multiplexing capabilities of the modified SPR instrument was pursued with the single-channel flow-cell design for which the laser line was coinciding with the flow path, allowing recording of SPR curves along a 10-mm length of the sensor surface. For that, sixteen positions (length, 0.3 mm; mutual distance, 0.3 mm) equally spaced along the channel were designated by the software for probing SPR signals. Subsequently, the full SPR curves for all sixteen spots of blank gold sensor surface were recorded simultaneously in the liquid media using 0.15 mM NaCl as running solvent. Similar SPR curves exhibiting the same dip angle were obtained for each spot, demonstrating uniform performance. In order to check the responses upon molecular adsorption to the gold surface, solutions of PEI, PSS, and PAH were successively flushed (4 min each) through the channel while recording SPR curves for all sixteen spots. Fig. 3a shows the obtained sensorgrams which reflect the consecutive polymer binding events. For all sixteen selected spots measured, similar resonance-angle shifts were observed for each applied layer. The baseline noise in the sensorgrams was 3.7 times higher for the multiplexed instrument as compared to the standard instrument, which probably is caused by the lower absolute intensity of the laser excitation per spot in the multiplexed system.

In order to verify the correct selection of the ROIs utilizing the camera, a PEI-PSS double layer and a PEI-PSS-PAH triple layer were adsorbed to two zones of the sensor surface, respectively, and the electrostatic binding of lysozyme (pI 11; positively charged) was monitored. Eight individual spots were selected for each of the zones using the software. First, a baseline was established for all 16 spots when exposed to 0.15 M NaCl only. Subsequently, a solution of lysozyme (1 mg/ml in 0.15 mM NaCl) was plug-injected for 1 min at 50 µl/min and SPR curves were recorded simultaneously for all spots. The resulting sensorgrams (Fig. 3b) recorded for the spots in the first zone (PEI-PSS) show typical protein binding curves, indicating significant interaction of lysozyme with the negatively charged layer. For the spots in the second zone (PEI-PSS-PAH), no change of SPR signal was observed, indicating no binding of lysozyme and confirming the effectiveness of such a triple layer as non-adsorptive coating for positively

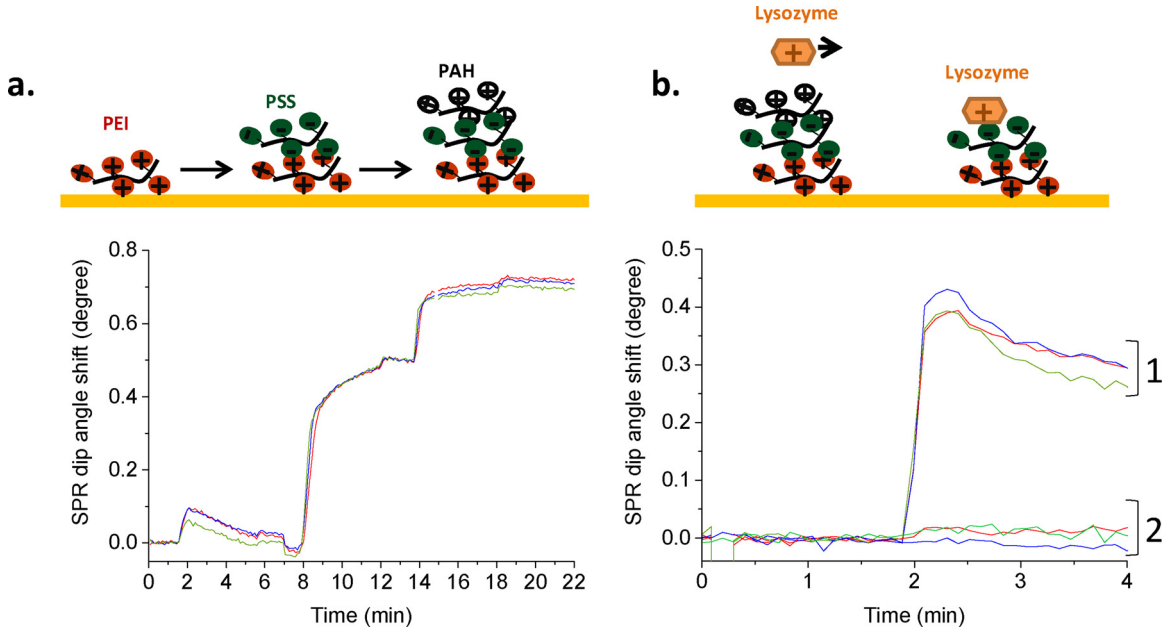


**Fig. 3.** Sensorgrams of **a.** online successive deposition of the polyelectrolytes indicated at the top, and **b.** injections of lysozyme on a sensor chip of which half of the spots comprised a PEI-PSS double layer (negatively charged; region 1) and the other half a PEI-PSS-PAH triple layer (positively charged; region 2).

charged proteins. These results indicate that each spot can be probed correctly by the multiplexed angular-scanning SPR instrument.

### *3.3. Antibody-protein interaction analysis by multiplexed angular-scanning SPR*

As a proof of principle for more practical SPR analyses, the potential of the multiplexed angular-scanning SPR system for the simultaneous monitoring of multiple biomolecular interactions was investigated. For that, the detection of the selective binding of antibodies with target proteins was used as a model test. Solutions (1 mg/ml each) of the target proteins HSA, hemoglobin, transferrin and cytochrome c in 5 mM MES hydrochloride (pH 4) were deposited in linearly aligned spots (length, 0.3 mm; mutual distance, 0.3 mm) on the surface of a CMD hydrogel gold sensor chip using a silicon mask with sixteen separate slits (see Section 2.5). Spots 1–5 were HSA, 6–10 were hemoglobin, 11–12 were blank (no protein applied), 13–14 were transferrin, and 15–16 were cytochrome c. Spots 11 and 12 were used for referencing the signals measured for the other spots (i.e. subtraction of the background signal caused by the sample solvent). The chip with the immobilized proteins was installed in the multiplexed SPR instrument. Fig. S1 shows full SPR curves of each spot could be measured simultaneously with the multiplexed system using the single channel flow cell. SPR curves recorded of the spots before protein immobilization (i.e. bare CMD surface) show very similar curves with resonance angles of 66.0°. Specific shifts of the resonance angle were observed for the respective immobilized proteins in the same figure.

Subsequently, using the single-channel flow cell, separate solutions of HSA and hemoglobin antibodies were successively injected (three times anti-HSA followed by three times anti-hemoglobin). Between protein injections, the sensor surface was regenerated with 50 mM NaOH for 1 min. SPR curves were continuously monitored for all spots. The sensorgrams obtained for the spots upon anti-HSA and anti-hemoglobin are shown in Fig. 4a and b, respectively (for raw data, see Fig. S2). Upon anti-HSA injection the five spots with immobilized HSA uniformly showed intense SPR responses, whereas no binding of anti-HSA was observed for the spots with immobilized hemoglobin, transferrin and cytochrome c (for transferrin and cytochrome c, see Fig. S2), indicating proper selectivity. For the hemoglobin-antibody injections, only specific binding was observed for the five hemoglobin spots which showed very similar sensorgrams. As a negative control, anti-myoglobin was sequentially injected in concentrations increasing from 0.1 to 100 µg/ml (six injections; Fig. 4c). Upon injection of the high concentration antibody, temporary increase of the signal was observed as a result of the bulk effect which in principle can be corrected with the reference channels signal (purple lines). Importantly, the simultaneously monitored sensorgrams showed no specific binding to any of the immobilized proteins, nicely confirming the suitability of the multiplexed SPR approach.

In order to study the potential of the multiplexed angular-scanning setup for measuring antibody-ligand binding characteristics, different concentrations of anti-HSA and anti-hemoglobin (0.1–100 µg/ml) were plug-injected in triplicate and sensorgrams were constructed from the SPR curves obtained for the HSA and hemoglobin spots (Fig. 5a and b, respectively). The figures show consistent performance of the various spots. For example, for 50 µg/ml anti-HSA, the average SDs within one spot and in between spots were 0.019 and 0.018°, respectively. For 50 µg/ml anti-hemoglobin, the average SDs within one spot and in between spots were 0.004 and 0.011°, respectively.

From the sensorgrams obtained, the association rate ($k_a$), dissociation rate ($k_d$) and dissociation ($K_D$) constants for the antibody-protein interactions were calculated using the BivalentInteraction model fitting in TraceDrawer software (Table S1). The kinetics calculation showed higher association rate and slower dissociation rate of the HSA antibody to HSA protein in comparison with the Hemoglobin antibody to hemoglobin protein. The $K_D$s obtained for the HSA-anti-HSA complex from the respective spots under the here introduced experimental conditions, were 34.1 ± 2.3 nM, 50.9 ± 2.7 nM, 55.1 ± 3.4 nM, 58.8 ± 4.2 nM and 61.7 ± 3.8 nM. For hemoglobin, the obtained $K_D$s were 21.2 ± 2.8 µM, 43.7 ± 3.0 µM, 44.3 ± 5.3 µM, 38.8 ± 3.0 µM and 56.7 ± 4.8 µM. The obtained $K_D$s show good repeatability within each spot and are similar for each antibody. Lower $K_D$ values indicate higher binding affinity of the HSA antibody to HSA protein, compare to hemoglobin antibody to hemoglobin protein.

In order to demonstrate the further applicability of the multiplexed angular-scanning SPR system for protein binding assays, antibodies were pre-incubated with their respective antigens and analyzed. A mixture of anti-hemoglobin and anti-HSA was plug-injected in the presence of increasing concentrations of HSA and hemoglobin and full SPR curves were recorded simultaneously for all immobilized protein

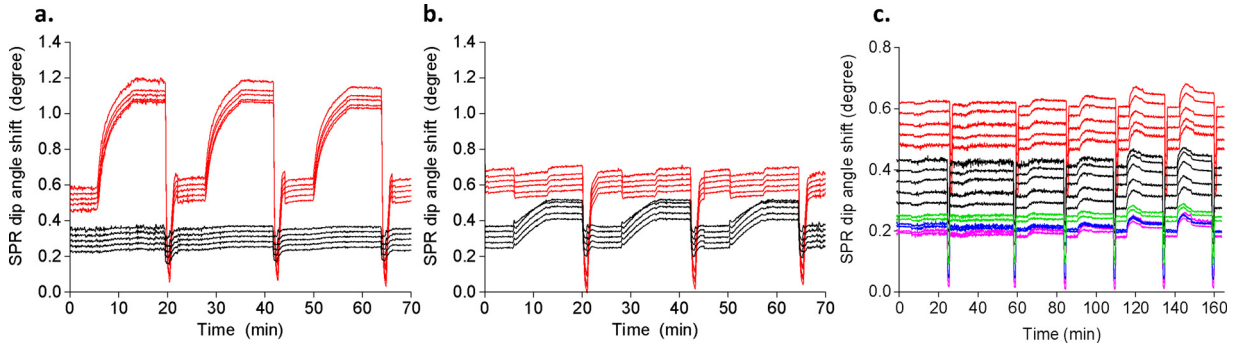


**Fig. 4.** Multiplexed angle-scanning SPR using a sensor with multiple immobilized proteins. Sensorgrams (baseline subtracted) for three consecutive plug-injections of **a.** anti-HSA and **b.** anti-hemoglobin. **c.** Sensorgrams (not baseline subtracted) for six consecutive plug-injections of anti-myoglobin at increasing concentration (0.1–100 μg/mL). Immobilized proteins: HSA (five spots; red lines), hemoglobin (five spots; black lines), transferrin (two spots; green lines), cytochrome c (two spots; blue lines), no protein (two spots; purple lines). Sensorgrams were given an intensity offset for clarity (avoiding overlap). (For interpretation of the references to colour in this figure legend, the reader is referred to the web version of this article).

spots. The binding events of high antibody concentrations with and without pre-incubation of antigenic proteins led to the sensorgram shown in Fig. S3. Sensorgrams of pre-incubation of antibodies with different concentrations of proteins for the HSA and hemoglobin positions are shown in Fig. 6a and b, respectively. SPR clearly showed a decrease of antibody binding with increasing concentrations of antigenic protein in the injected incubation mixture. Results showed similar curve shape and affinity in between the spots, which confirms the reproducibility of the system in between spots for biomolecular interaction analysis. From the obtained sensorgrams for each respective spot, the IC50 values for the antigens were determined, yielding 155 ± 3 nM, 143 ± 15 nM, 157 ± 23 nM, 145 ± 11 nM and

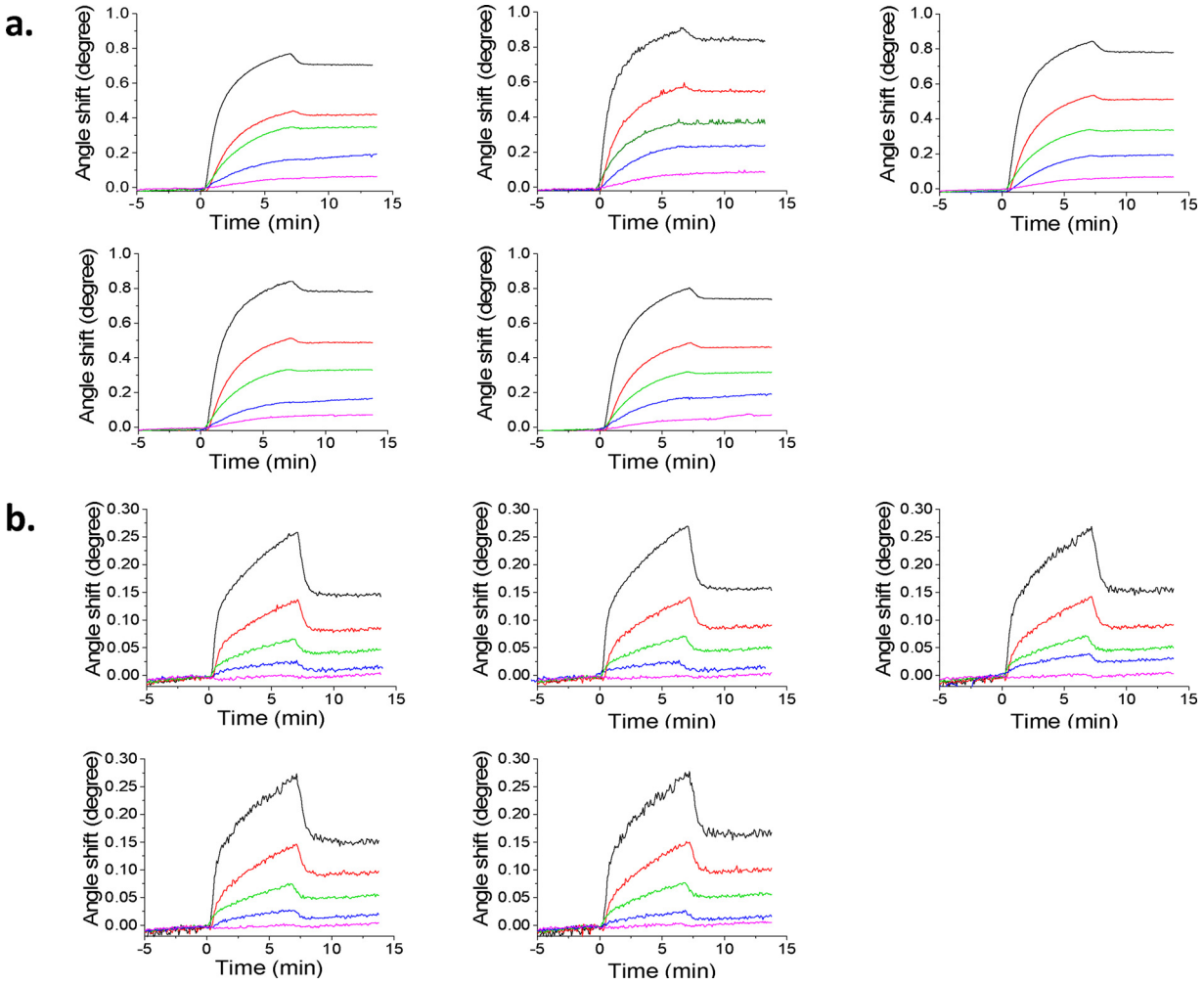


**Fig. 5.** Multiplexed angle-scanning SPR using a sensor with multiple immobilized proteins. Sensorgrams for **a.** the five HSA spots upon exposure to increasing concentrations of anti-HSA, and **b.** the five hemoglobin spots upon exposure to increasing concentrations of anti-hemoglobin. Antibody concentrations: 1 (purple), 10 (blue), 25 (green), 50 (red) and 100 (black) μg/ml (For interpretation of the references to colour in this figure legend, the reader is referred to the web version of this article).

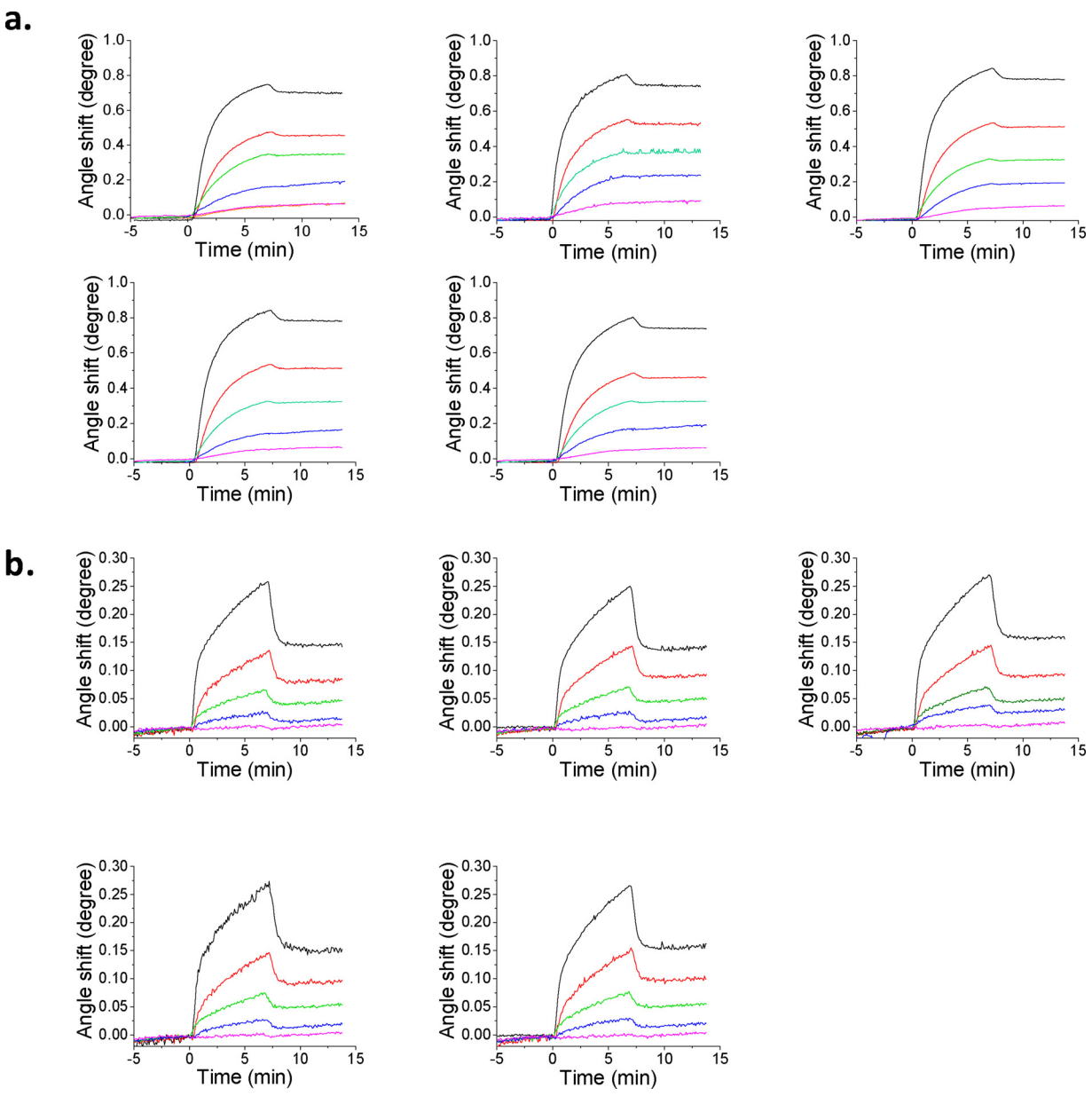


**Fig. 6.** Multiplexed angle-scanning SPR using a sensor with multiple immobilized proteins. Sensorgrams for **a.** the five HSA spots upon exposure to anti-HSA (200 µg/ml) incubated with different concentrations of HSA, and **b.** the five hemoglobin spots upon exposure to increasing anti-hemoglobin antibody (200 µg/ml) incubated with different concentrations of hemoglobin. Protein-ligand concentrations: 100 (purple), 50 (blue), 25 (green), 10 (red) and 1 (black) µg/mL (For interpretation of the references to colour in this figure legend, the reader is referred to the web version of this article).

156 ± 24 nM for HSA, and 73.1 ± 2.4 nM, 75.3 ± 1.0 nM, 75.3 ± 1.3 nM, 75.0 ± 2.1 nM and 74.1 ± 1.5 nM for hemoglobin.

## 4. Conclusions

This study presents the development of a multiplexed line-laser based angular-scanning SPR system with a Kretschmann configuration allowing binding evaluation and measurement of multiple analytes and/or ligands simultaneously. Continuous angular scanning between 40–75° provided full SPR curves for the complete sensor area covered by the laser line. This wide angular range permits SPR measurements in both air and liquid media. Flow cells with six parallel channels or a single channel with up to sixteen detection spots were utilized for multiplexed analysis. The basic performance of the new setup was tested monitoring responses by ethanol refractive index changes, protein adsorption and polyelectrolyte-layer adsorption. The results showed the capability of the newly developed system for performing reliable multiplex analyses. Applicability for biosensing was shown by multiplexed measuring antibody-antigenic protein interactions. Several proteins were immobilized in up to sixteen discrete spots in line on the surface of a CMD hydrogel gold sensor chip. Analysis of (mixtures of) antibodies provided a simultaneous assessment of binding to each of the immobilized antigens, showing excellent selectivity, repeatability and reproducibility among the probed spots. Obtained full SPR curves and sensorgrams allowed calculation of binding-kinetic and inhibition constants ($k_a$, $k_d$, $K_D$, IC50). The here presented system substantially increases the throughput of full angle scanning SPR in single flow channel format. In theory, the presented system will allow extension of multiplexed SPR detection of approximately up to 100 ROIs (20-pixel lines per ROI). For that, advanced offline techniques for accurate ligand immobilization on the surface of SPR sensor should be used.

## Conflicts of interest

The authors declare no conflicts of interest.

## Acknowledgments

This research is funded by Netherlands Organization for Scientific Research (NWO) in the framework of Technology Area COAST (project nr 053.21.107) with Wageningen University, RIKILT, Heineken, Synthon, Technex, EuroProxima, Waterproef as partners and BioNavis and Plasmore as associated partners.

## Appendix A. Supplementary data

Supplementary material related to this article can be found, in the online version, at doi:https://doi.org/10.1016/j.snb.2018.11.046.

## References

[1] M.A. Cooper, Label-free screening of bio-molecular interactions, Anal. Bioanal. Chem. 377 (2003) 834–842, https://doi.org/10.1007/s00216-003-2111-y377 834 (2003).
[2] H.R. Gwon, S.H. Lee, Spectral and angular responses of surface plasmon resonance based on the Kretschmann prism configuration, Mater. Trans. 51 (2010) 1150–1155, https://doi.org/10.2320/matertrans.M2010003.
[3] G. Schröder, E. Lanka, TraG-like proteins of type IV secretion systems: functional dissection of the multiple activities of TraG (RP4) and TrwB (R388), J. Bacteriol. 185 (2003) 4371–4381, https://doi.org/10.1128/JB.185.15.4371-4381.2003.
[4] P. Säfsten, S.L. Klakamp, A.W. Drake, R. Karlsson, D.G. Myszka, Screening antibody-antigen interactions in parallel using Biacore A100, Anal. Biochem. 353 (2006) 181–190, https://doi.org/10.1016/j.ab.2006.01.041.
[5] R. Otupiri, E.K. Akowuah, S. Haxha, Multi-channel SPR biosensor based on PCF for multi-analyte sensing applications, Opt. Express 23 (2015) 15716–15727, https://doi.org/10.1364/OE.23.015716.
[6] S. Joshi, A. Segarra-Fas, J. Peters, H. Zuilhof, T.A. van Beek, M.W. Nielen, Multiplex surface plasmon resonance biosensing and its transferability towards imaging nanoplasmonics for detection of mycotoxins in barley, Analyst 141 (2016) 1307–1318, https://doi.org/10.1039/C5AN02512E.
[7] G. Steiner, Surface plasmon resonance imaging, Anal. Bioanal. Chem. 379 (2004) 328–331, https://doi.org/10.1007/s00216-004-2636-8.
[8] S. Joshi, P. Pellacani, T.A. van Beek, H. Zuilhof, M.W.F. Nielen, Surface characterization and antifouling properties of nanostructured gold chips for imaging surface plasmon resonance biosensing, Sens. Actuators B Chem. 209 (2015) 505–514, https://doi.org/10.1016/j.snb.2014.11.133.
[9] C. Zhou, W. Jin, Y. Zhang, M. Yang, L. Xiang, Z. Wu, et al., An angle-scanning surface plasmon resonance imaging device for detection of mismatched bases in caspase-3 DNA, Anal. Methods 5 (2013) 2369–2373, https://doi.org/10.1039/C3AY26602H.
[10] J.B. Beusink, A.M. Lokate, G.A. Besselink, G.J. Pruijn, R.B. Schasfoort, Angle-scanning SPR imaging for detection of biomolecular interactions on microarrays, Biosens. Bioelectron. 23 (2008) 839–844, https://doi.org/10.1016/j.snb.2010.04.015.
[11] C. Yu, J. Irudayaraj, Quantitative evaluation of sensitivity and selectivity of multiplex nanoSPR biosensor assays, Biophys. J. 93 (2007) 3684–3692, https://doi.org/10.1529/biophysj.107.110064.
[12] S. Scarano, M. Mascini, A.P.F. Turner, M. Minunni, Surface plasmon resonance imaging for affinity-based biosensors, Biosens. Bioelectron. 25 (2010) 957–966, https://doi.org/10.1016/j.bios.2009.08.039Reference:BIOS 3445.
[13] B.D. Brooks, A.R. Miles, Y.N. Abdiche, High-throughput epitope binning of therapeutic monoclonal antibodies: why you need to bin the fridge, Drug Discov. Today 19 (2014) 1040–1044, https://doi.org/10.1016/j.drudis.2014.05.011.
[14] Y.N. Abdiche, R. Harriman, X. Deng, Y.A. Yeung, A. Miles, W. Morishige, et al., Assessing kinetic and epitopic diversity across orthogonal monoclonal antibody generation platforms, MAbs 8 (2016) 264–277, https://doi.org/10.1080/19420862.2015.1118596.
[15] Y.N. Abdiche, A. Miles, J. Eckman, D. Foletti, T.J. Van Blarcom, Y.A. Yeung, et al., High-throughput epitope binning assays on label-free array-based biosensors can yield exquisite epitope discrimination that facilitates the selection of monoclonal antibodies with functional activity, PLoS One 9 (2014) e92451, , https://doi.org/10.1371/journal.pone.0092451.
[16] J.J. van Beers, R. Raijmakers, L.E. Alexander, J. Stammen-Vogelzangs, A.M. Lokate, A.J. Heck, et al., Mapping of citrullinated fibrinogen B-cell epitopes in rheumatoid arthritis by imaging surface plasmon resonance, Arthritis Res. Ther. 12 (2010), https://doi.org/10.1186/ar3205 R219, Epub 2010 Dec 23.
[17] K.P. Geuijen, R.B. Schasfoort, R.H. Wijffels, M.H. Eppink, High-throughput and multiplexed regeneration buffer scouting for affinity-based interactions, Anal. Biochem. 454 (2014) 38–40, https://doi.org/10.1016/j.ab.2014.03.011 Epub 2014 Mar 21.
[18] D. Dorokhin, W. Haasnoot, M.C. Franssen, H. Zuilhof, M.W. Nielen, Imaging surface plasmon resonance for multiplex microassay sensing of mycotoxins, Anal. Bioanal. Chem. 400 (2011) 3005–3011, https://doi.org/10.1007/s00216-011-4973-8.
[19] R.B.M. Schasfoort, A.J. Tudos, Handbook of Surface Plasmon Resonance, Royal Society of Chemistry, 2008.